Analytical Biochemistry 463 (2014) 7–14

Contents lists available at ScienceDirect

Analytical Biochemistry

journal homepage: www.elsevier.com/locate/yabio

Surface plasmon resonance sensor for femtomolar detection of testosterone with water-compatible macroporous molecularly imprinted film

Qingwen Zhang [a], Lijing Jing [a], Jinling Zhang [b], Yamin Ren [a], Yang Wang [a], Yi Wang [b,*], Tianxin Wei [a,*], Bo Liedberg [b]

[a] Key Laboratory of Cluster Science of Ministry of Education, Beijing Institute of Technology, Beijing 100081, China
[b] Centre for Biomimetic Sensor Science, Nanyang Technological University, Singapore 637553, Singapore

ARTICLE INFO

Article history:
Received 3 April 2014
Received in revised form 20 June 2014
Accepted 21 June 2014
Available online 30 June 2014

Keywords:
Molecularly imprinted film (MIF)
Testosterone
Water-compatible
Surface plasmon resonance (SPR)
Sensor
Macroporous film

ABSTRACT

A novel water-compatible macroporous molecularly imprinted film (MIF) has been developed for rapid, sensitive, and label-free detection of small molecule testosterone in urine. The MIF was synthesized by photo copolymerization of monomers (methacrylic acid [MAA] and 2-hydroxyethyl methacrylate [HEMA]), cross-linker (ethylene glycol dimethacrylate, EGDMA), and polystyrene nanoparticles (PS NPs) in combination with template testosterone molecules. The PS NPs and template molecules were subsequently removed to form an MIF with macroporous structures and the specific recognition sites of testosterone. Incubation of artificial urine and human urine on the MIF and the non-imprinted film (NIF), respectively, indicated undetectable nonspecific adsorption. Accordingly, the MIF was applied on a surface plasmon resonance (SPR) sensor for the detection of testosterone in phosphate-buffered saline (PBS) and artificial urine with a limit of detection (LOD) down to 10^{-15} g/ml. To the best of our knowledge, the LOD is considered as one of the lowest among the SPR sensors for the detection of small molecules. The control experiments performed with analogue molecules such as progesterone and estradiol demonstrated the good selectivity of this MIF for sensing testosterone. Furthermore, this MIF-based SPR sensor shows high stability and reproducibility over 8 months of storage at room temperature, which is more robust than protein-based biosensors.

Molecular imprinting is a well-established technique for the preparation of polymers with specific recognition sites of molecules [1,2] and cells [3] on various applications [4,5], including artificial antibodies [6,7], chromatographic separations [8], sensors [9,10], and mimic enzyme catalysis [11,12]. In general, molecularly imprinted polymers (MIPs)[1] are prepared by copolymerization of functional monomers and cross-linkers at the presence of template molecules in a porogen solvent. After the subsequent removal of the templates from polymer matrix, complementary cavities in memory of size, shape, and orientation of their binding sites to the target molecules are formed. The previously developed MIPs have demonstrated robustness and high selectivity for the recognition of target molecules predominantly in organic solvent media [13–15]. However, the MIPs employed for selective binding targets in aqueous conditions is an issue that should be addressed because many target molecules of interest are present only in aqueous solution such as body fluids, drinks, and waste water. Therefore, it is necessary to develop water-compatible MIPs for binding the targets in a specific and selective manner [16–19]. The major challenge on the preparation of MIPs with high selectivity in aqueous media is to overcome the nonspecific hydrophobic binding of targets that is often induced by water. To achieve this, various approaches have been used, including tuning the polarities of porogens and incorporating polar or nonpolar comonomers or cross-linkers into the MIP matrix [20]. In addition, MIPs with macroporous structures such as inverse opal structure have been fabricated for label-free detection of small molecules in water medium [21,22]. These macrostructures provides high accessibility for molecules binding into the polymer

* Corresponding authors. Fax: +65 67912274 (Y. Wang), +86 10 68945482 (T. Wei).
E-mail addresses: yiwang@ntu.edu.sg (Y. Wang), txwei@bit.edu.cn (T. Wei).

[1] *Abbreviations used:* MIP, molecularly imprinted polymer; PS NP, polystyrene nanoparticle; SPR, surface plasmon resonance; MIF, molecularly imprinted film; UV, ultraviolet; NIF, non-imprinted film; PBS, phosphate-buffered saline; LOD, limit of detection; HEMA, 2-hydroxyethyl methacrylate; EGDMA, ethylene glycol dimethacrylate; MAA, methacrylic acid; AU, artificial urine; SAM, self-assembled monolayer; SP, surface plasmon; SEM, scanning electron microscope; ELISA, enzyme-linked immunosorbent assay.

http://dx.doi.org/10.1016/j.ab.2014.06.014
0003-2697/

matrices. However, this sensor relying on the diffraction or color changes of the thick MIPs has limited sensitivity. Here we have developed a procedure for the preparation of water-compatible MIPs by introducing monomer with high polarity and a macroporous structure by removing polystyrene nanoparticles (PS NPs) from the polymers. The MIPs with thickness of approximately 180 nm, which is comparable to the penetration depth of surface plasmon resonance (SPR), were well-controlled and synthesized in situ on an SPR sensor chip. This functionalized SPR sensor chip was further employed for the specific detection of testosterone in aqueous solution.

SPR is an optical phenomenon that enables the detection of mass changes on the surface of metallic substrates. It has been widely developed as a rapid, label-free, and real-time assay technique for highly sensitive detection of chemical and biological analytes [23], including large molecules such as antibodies [24], protein [25,26], pathogen [27], and nucleic acids [28]. SPR has also been reported for the detection of small molecules with high sensitivity. For instance, SPR sensors enable the detection of hormone at the picogram per milliliter (pg/ml) range [29] and trinitrotoluene (TNT) down to tens of femtomoles (fM) based on the molecularly imprinted gold nanoparticles [30]. Testosterone is a steroid hormone that acts as an indicator of a great many pathological conditions such as a prostate cancer biomarker and a stimulant that is often illegally used to increase muscle mass and strength in athletic sports. In general, the daily production rates of testosterone are 4 to 12 mg in young men and 0.5 to 2.9 mg in young women [31]. Conventional testosterone analysis is performed by immunoassays [32,33] and chromatography [34,35]. The immunoassays typically provide high sensitivity but require long incubation/washing steps and rely on the antibodies that have limited thermal stability, whereas the chromatography suffers from the weak specificity and insufficient sensitivity. SPR sensors in combination with MIPs can address this issue for the detection of small molecules at high sensitivity and selectivity [36,37]. In addition, an SPR sensor chip with a three-dimensional binding matrix such as hydrogel and MIPs containing a porous structure could improve the sensitivity because it provides higher binding capacity [38] and allows the target molecules to diffuse rapidly to the recognition sites.

In this study, a water-compatible macroporous molecularly imprinted film (MIF) was prepared on an SPR sensor chip through ultraviolet (UV) photo-polymerization. The macroporous structure of the MIF was developed through removal of PS NPs from the polymerized MIPs. The MIF with a high porosity was expected to provide a high capacity and high accessibility for the target molecules reaching to the recognition binding sites, thereby resulting in high sensitivity for rapid detection of the corresponding targets. The selectivity of the MIF was investigated on two other analogues, namely estradiol and progesterone. Furthermore, the nonspecific adsorption of serum, artificial urine, and human urine was evaluated on macroporous MIF and non-imprinted films (NIFs), respectively. This macroporous MIF was finally used for SPR sensing of testosterone in phosphate-buffered saline (PBS) buffer and artificial urine with a limit of detection (LOD) down to 10^{-15} g/ml. The sensor performance of the MIF in female and male human urine was also investigated. In addition, the stability and reproducibility of this SPR sensor chip were investigated after 8 months of storage at room temperature.

Materials and methods

Materials

Testosterone (MW = 288.42, cat. no. A0277793) and benzophenone (BP, wt% = 99%, cat. no. A0253552) were purchased from Acros Organics (China). 17β-Estradiol (cat. no. 11657, wt% = 98%), progesterone (USP, cat. no. 15925), 2-hydroxyethyl methacrylate (HEMA, wt% = 96%), and ethylene glycol dimethacrylate (EGDMA, analytical grade, wt% = 98%) were purchased from Aladdin Reagent (China). PS NPs (100 nm, 25 mg/ml, cat. no. 619820) were purchased from Polysciences (Germany). Methacrylic acid (MAA, analytical grade, wt% = 99%) and 1-dodecanethiol (wt% = 98%, cat. no. LBB0J03) were purchased from J & K Scientific (China). PBS was prepared from 140 mM NaCl, 10 mM phosphate, and 3 mM KCl, and pH 7.4 was adjusted by HCl and NaOH. Ethanol, acetic acid, and acetone were all analytical grade and purchased from Beijing Tongguang Fine Chemicals (China). MAA, HEMA, and EGDMA were distilled under reduced pressure before use. All of the other reagents were used as received. Rabbit serum was purchased from Sigma–Aldrich (cat. no. R9133, Singapore). Artificial urine (AU) solution at pH 6.0 was prepared by dissolving 2.0 mM citric acid, 25 mM $NaHCO_3$, 170 mM urea, 2.5 mM $CaCl_2$, 90 mM NaCl, 2.0 mM $MgSO_4$, 10 mM Na_2SO_4, 7 mM KH_2PO_4, 7 mM K_2HPO_4, and 25 mM NH_4Cl in water [39]. The pH of the solution was adjusted to 6.0 by the addition of 1.0 M HCl. Human urine samples were obtained from female and male volunteers.

Sensor surface functionalized with macroporous MIF

First, the gold chip was immersed in 1 mM 1-dodecanethiol ethanol solution for 24 h to form a self-assembled monolayer (SAM), which will react with the benzophenone to form free radicals for anchoring polymers. The testosterone-imprinted film was synthesized based on UV photo polymerization. Next, 0.036 g of testosterone was mixed with 42 μl of MAA and 61 μl of HEMA in 4.518 ml of ethanol. The mixture was sonicated for 20 min and pre-polymerized for 4 h at room temperature. Subsequently, the mixture was added to 355 μl of cross-linker EGDMA, 25 μl of PS NPs, and 0.02 g of benzophenone as initiator. After being treated with nitrogen gas for 10 min, the reaction solution was injected into a homemade flow cell in contact with the SAM modified gold chip for in situ polymerization. The thin MIF embedded with PS NPs (PS–MIF) was formed on the gold chip by UV irradiation (λ = 365 nm, irradiation power of 2 W/cm^2). The formation of the MIF on gold chip was real-time monitored by SPR reflectivity changes and the angular spectra. Afterward, the PS NPs were removed from PS–MIF by rinsing with acetone overnight to form the macroporous film. Finally, the macroporous MIF was rinsed with a mixture of ethanol and acetic acid (v/v = 1:1) to remove the template molecule testosterone from the MIF and form the recognition cavities. For a blank control, a macroporous NIF was prepared through removal of PS NPs from the same polymers without imprinting of template molecules. In addition, a conventional MIF was synthesized through the polymerization of the same monomers and template molecules but without PS NPs. The thickness of the MIF was determined with Alpha Step IQ Surface Profiler (KLA-Tencor, Milpitas, CA, USA) by carefully scratching the film with a needle to form a scratch down to the glass with approximately 100 μm in width. The underneath gold film with a thickness of 50 nm was taken into account.

SPR implementation

In the experiment, an optical setup based on SPR spectroscopy was employed [40] (Fig. 1). A light beam emitted from a stabilized HeNe laser (2 mW, λ = 632.8 nm) passed through a polarizer to become a transverse magnetically polarized beam and was coupled to a LASFN 9 glass prism (90°, n_p = 1.845) with an optically matched sensor chip to its base by using immersion oil. A flow cell with a volume of approximately 0.5 ml was pressed against the sensor surface to flow liquid sample over the substrate surface

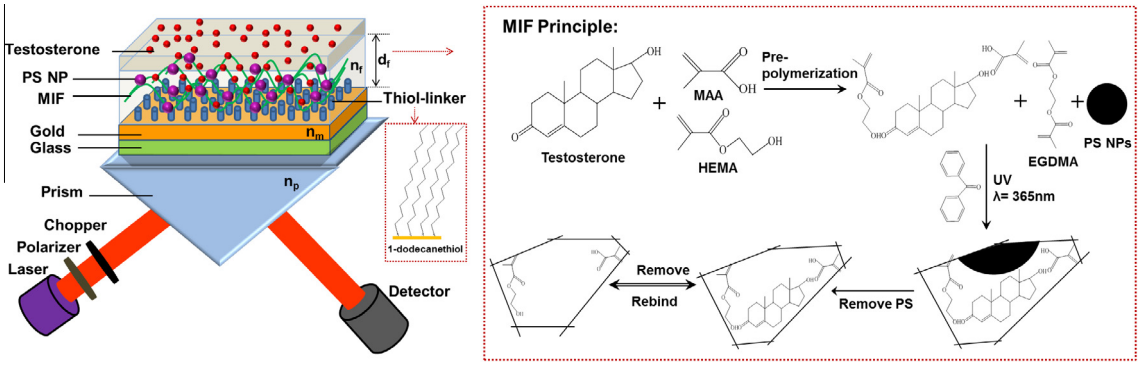

Fig.1. Scheme of SPR sensor setup, the PS–MIF functionalized sensor chip, and the procedure for the formation of macroporous MIF.

with a peristaltic pump at a flow rate approximately 0.25 ml/min. The excitation of surface plasmon (SP) was observed from the angular reflectivity spectra measured by using a photodiode detector and a rotation stage. The resonant coupling of an incident light beam to SP is manifested as resonant dips in the reflectivity spectra. To evaluate the property of the MIF, the angular reflectivity spectra were fitted by a transfer matrix-based model that was implemented in the software Winspall (developed at the Max Planck Institute for Polymer Research, Mainz, Germany). The parameters were fitted as follows: refractive index of prism $n_p = 1.845$, thickness of $d_m = 41.5$ nm, refractive index of $n_m = 0.2+3.5144i$ for gold film, refractive index of ethanol $n_{b1} = 1.3582$, and refractive index of PBS $n_{b2} = 1.3338$. The surface coverage of the MIF and testosterone molecules was estimated according to the following equation [41]:

$$\Gamma = \frac{(n_f - n_b)d_f}{\partial n/\partial c}, \quad (1)$$

where n_b and n_f are the refractive index of a sample solution and the MIF, respectively, and d_f is the thickness of the MIF. The factor of $\partial n/\partial c = 0.2$ mm^3/mg relates the refractive index changes with concentration variations of molecules such as proteins and small organic molecules and was taken from the literature [42,43].

Detection of testosterone

The macroporous MIF with recognition cavities was immersed in PBS buffer and AU for the monitoring of testosterone. Samples were prepared by spiking the PBS buffer or AU with testosterone at concentrations ranging from 10^{-15} to 10^{-7} g/ml. Afterward, each sample with a volume of 0.8 ml was pumped through the sensor surface and circulated during the incubation for 20 min, followed by rinsing of the sensor surface with PBS buffer or AU for approximately 10 min. To investigate the selectivity of the MIF, two analogue molecules, estradiol and progesterone, at a concentration of 10^{-6} g/ml in PBS buffer were respectively incubated with the MIF. For the control experiment, the testosterone of 10^{-6} g/ml in PBS buffer was incubated with the macroporous NIF and conventional MIF.

Results and discussion

Preparation and characterization of macroporous MIF

The water-compatibility and unspecific binding properties of MIF are strongly correlated to the polarity of porogen and monomers. It has been reported that MIPs containing HEMA showed improved specific binding of L-nicotine in water as compared with MIF made with only MAA monomer [20]. However, the high amount of HEMA may also result in high unspecific binding of MIPs. Here, MAA and HEMA at a concentration ratio of 1:1 were employed for the development of MIPs where the specific recognition sites were formed through the hydrogen bonds among the hydroxyl/carbonyl groups in testosterone and the carboxyl and hydroxyl groups in MAA and HEMA, respectively (Fig. 1). The optimization of experimental condition for the preparation of the macroporous MIF is partially shown in Table S1 of the online supplementary material. The scanning electron microscope (SEM) image (Fig. 2A) indicated a highly dense MIF embedded with

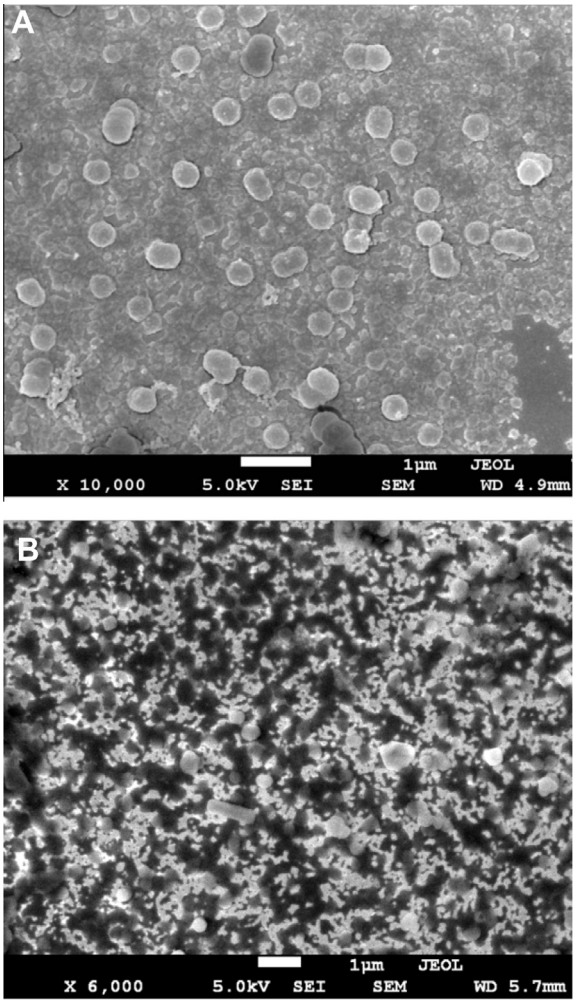

Fig.2. SEM images of MIF embedded with PS NPs (A) and the macroporous MIF after removal of PS NPs (B). Scale bars = 1 μm.

nanoparticles with diameters from 100 to 300 nm that are related to the PS NPs and their aggregates. A macroporous MIF with pores up to 2 μm in size was formed by removing the PS NPs from the MIF (Fig. 2B). The larger pores may partially be ascribed to the loss of monomers along with the removal of PS NPs.

The thickness of the MIF was controlled by stopping the UV radiation when the SPR resonant angle shifts to around 71°. For instance, the SPR resonant dip shifts from 60.2 to 71.7° (see Fig. 3A), indicating the formation of PS–MIF with a thickness of approximately $d_f = 177$ nm as measured by the Surface Profiler. The thickness of the film is comparable to the penetration depth of SPR; thus, the molecular binding in the whole film can be probed by the electromagnetic field of SPR. By fitting the spectra curve in Fig. 3A, the refractive index of PS–MIF was estimated as $n_f = 1.4505$ in ethanol. The mass coverage of PS–MIF on the gold substrate was estimated as $\Gamma_f = 81.7$ ng/mm^2 according to Eq. (1). The resonant angle of the PS–MIF was decreased by 0.35° after removal of PS NPs through rinsing with acetone solution overnight. The surface coverage of the removed PS NPs, accordingly, was evaluated as 1.4 ng/mm^2, which corresponds to approximately 3 particles/μm^2 (PS NPs have a mass of 1.82×10^{12} particles/mg according to the Polysciences data sheet). The PS coverage is comparable to the number of particles as indicated in the SEM imaging (Fig. 2A). To remove the template molecules from the MIF, acidic molecules were typically employed to break the hydrogen bonds between templates and the polymer [44]. Here, a mixture of ethanol and acetic acid (v/v = 1:1) was employed to remove the template molecules, resulting in a decrease of the resonant angle from 71.35 to 70.60° and a reflectivity decrease of $\Delta R = 7.5\%$ (Fig. 3A; see also Fig. S1a in supplementary material). Accordingly, we estimated the refractive index of the macroporous MIF as $n_f = 1.4448$ and the surface coverage of removed testosterone as $\Gamma = 5$ ng/mm^2, which is approximately 6.2% mass of the MIF. This result is comparable to the mass percentage of testosterone (7%) added in the polymer solution before polymerization. A comparison experiment on measuring the removal of template molecule from the conventional MIF (i.e., the MIF without incorporation of PS NPs during photo polymerization) showed negligible changes on the reflectivity and the resonant angles (Figs. S1b and S2). This is ascribed to the fact that the density of the conventional MIF was too high; thus, it is hard to remove the testosterone from the polymer network.

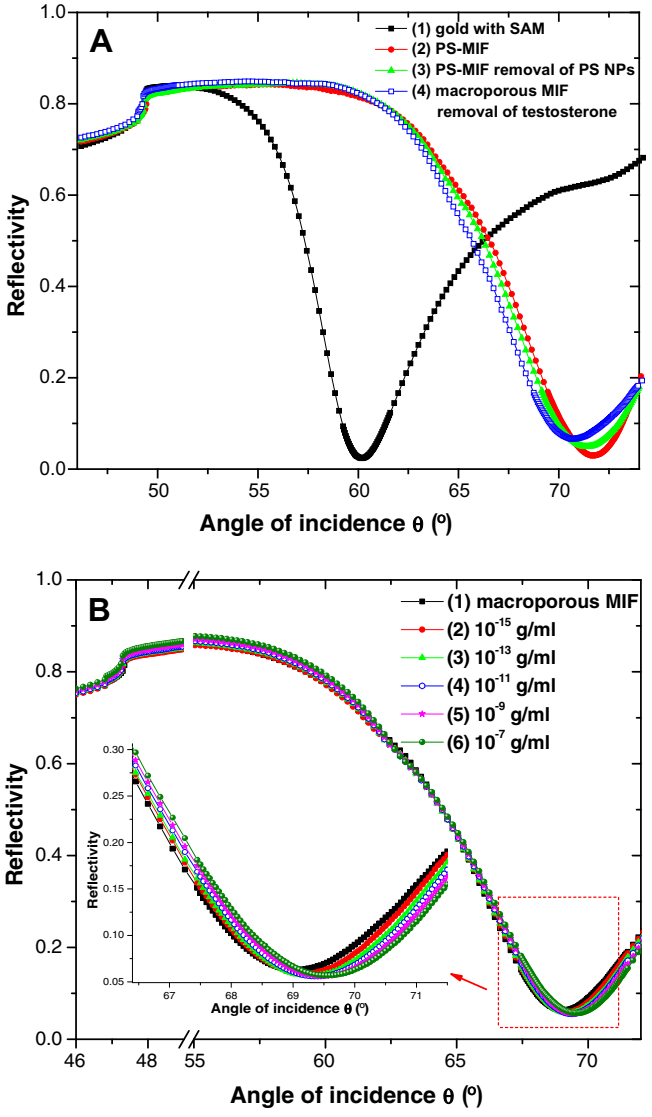

Fig.3. (A) Angular reflectivity spectra of gold film modified with SAM (1), functionalized with the PS–MIF (2), after the removal of PS NPs from the PS–MIF (3), and after the removal of testosterone as measured in ethanol (4). (B) Angular reflectivity spectra of the macroporous MIF on the affinity binding of testosterone at concentrations of 0 g/ml (1), 10^{-15} g/ml (2), 10^{-13} g/ml (3), 10^{-11} g/ml (4), 10^{-9} g/ml (5), and 10^{-7} g/ml (6) in PBS buffer.

Investigation of macroporous MIF for detection of testosterone

In further experiments, a time-dependent reflectivity changes ΔR was measured at an incident angle lower than the resonance angle with the highest slope $dR/d\theta$ (e.g., 67.5° for macroporous MIF). Affinity binding of testosterone molecules to the macroporous MIF was investigated on injecting a series of testosterone PBS solutions at the concentrations from 10^{-15} to 10^{-7} g/ml. The SPR resonance angle shifted to higher angles on the binding of testosterone (Fig. 3B). For instance, it increased from 69.00 to 69.12° after the incubation of testosterone at a concentration of 10^{-15} g/ml in PBS buffer solution (Fig. 3B). The time-dependent reflectivity changes showed an increase of reflectivity $\Delta R = 2.9\%$ after the incubation of a series of testosterone samples at concentrations up to 10^{-7} g/ml (Fig. 4A). The selectivity of the macroporous MIF was investigated by injecting testosterone analogue molecules such as progesterone and estradiol at a concentration of 10^{-6} g/ml in PBS. The reflectivity increased significantly on the injection of the samples as ascribed to the diffusion of the analogue molecules into the macroporous MIF. However, the reflectivity recovered after rinsing with PBS buffer. The reflectivity change $\Delta R = 0.23\%$ for the incubation of progesterone was one order of magnitude lower than the specific binding of testosterone ($\Delta R = 2.16\%$) at the same concentration (Fig. 4B). Compared with progesterone, the incubation of estradiol was accompanied by a relatively higher reflectivity changes $\Delta R = 0.52\%$. This might be ascribed to the more similar structure of estradiol, which has a hydroxyl group instead of a carbonyl group at position 3 (Fig. 4B), even though the reflectivity changes for the unspecific binding of estradiol was still more than 4-fold lower than the affinity binding of testosterone. The result indicates that testosterone-imprinted macroporous MIF has good selectivity to the recognition of testosterone molecules. As a comparison, a conventional MIF was also employed to investigate the affinity binding between the testosterone and the MIF. A negligible change ($\Delta R = 0.07\%$) was observed for the binding of testosterone to the conventional MIF at a concentration of 10^{-6} g/ml in PBS (Fig. 4B). The 30-fold lower response than that on macroporous MIF is ascribed to the high density of the conventional MIF; thus, only few recognition sites are accessible in the MIF. These results indicated that the high porosity of MIF could significantly improve the accessibility and sensitivity for the binding of testosterone.

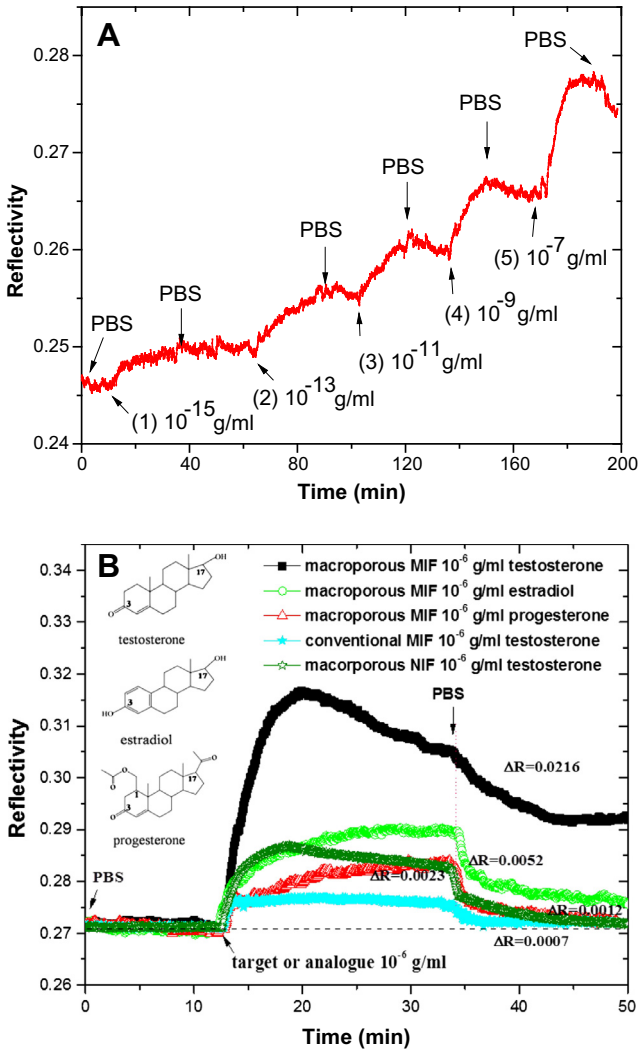

Fig.4. (A) Time-dependent SPR reflectivity changes due to the affinity binding of testosterone at concentrations of 10^{-15} g/ml (1), 10^{-13} g/ml (2), 10^{-11} g/ml (3), 10^{-9} g/ml (4), and 10^{-7} g/ml (5) in PBS buffer. The sensor chips were rinsed with pure PBS buffer between each binding cycle. (B) Time-dependent reflectivity changes for the macroporous MIF on the injection of testosterone, progesterone, and estradiol at a concentration of 10^{-6} g/ml in PBS, respectively, as well as for the conventional MIF and macroporous NIF incubated with 10^{-6} g/ml testosterone. The inset shows the chemical structures of testosterone, progesterone, and estradiol.

A control experiment on the incubation of a blank macroporous NIF (without testosterone during polymerization) in a 10^{-6} g/ml testosterone PBS solution showed reflectivity changes of $\Delta R = 0.12\%$ on the SPR measurement (Fig. 4B). The response is comparable to the reflectivity changes for the binding of analogue molecules (i.e., progesterone and estradiol) on the macroporous MIF. The results indicated that there were no specific recognition sites for testosterone in the control NIF, and the response is ascribed to the nonspecific interaction between the molecules and the polymer matrix. However, this unspecific response in macroporous NIF is higher than the specific response of testosterone on the conventional MIF $\Delta R = 0.07\%$ (Fig. 4B), indicating that the macroporous structure provides both more specific and nonspecific interactions between testosterone and the polymer matrix.

Unspecific adsorption of serum, artificial urine, and human urine

The unspecific interaction of serum and AU with the macroporous MIF was investigated to evaluate the potential analysis of testosterone in these samples. Fig. 5A shows the reflectivity curves measured on the incubation of the macroporous MIF with serum at concentrations of 10, 50, and 100%. These data reveal that after the flows of 50 and 100% serum, the reflectivity at an incident angle of 70° increased significantly due to the high refractive index of serum. The reflectivity changes before and after the incubation with 10, 50, and 100% serum are $\Delta R = 0.20$, 0.75, and 2.25%, respectively. These reflectivity changes at 50 and 100% serum are much higher than the affinity binding of testosterone at concentrations lower than 10^{-13} g/ml (Fig. 4A). The angular reflectivity spectra also show the angular shifts of approximately $\Delta\theta = 0.2°$ after incubation with 100% serum (Fig. 5A). The high unspecific binding of serum in the macroporous MIF reveals the unfeasibility to detect the testosterone in 50 or 100% serum. However, the incubation of AU on the sensor chip shows undetectable reflectivity changes, indicating negligible nonspecific binding of AU in the macroporous MIF (Fig. 5B). The reflectivity increases after the incubation of AU was due to the increased refractive index of AU (see Fig. S3 in supplementary material), and later the decrease of the reflectivity

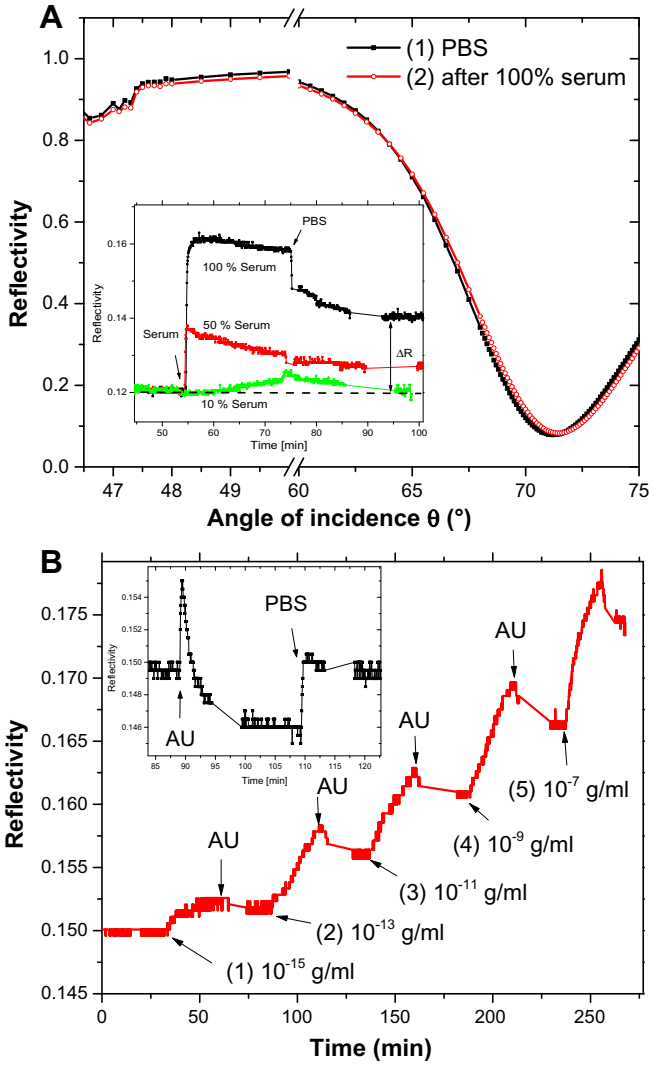

Fig.5. (A) Angular reflectivity of the macroporous MIF before (1) and after (2) being incubated with 100% serum as measured in PBS. The inset shows the kinetics of the reflectivity signal on injections of 10, 50, and 100% serum as measured at 70°. (B) Reflectivity kinetics on the binding of testosterone on the macroporous MIF at concentrations from 10^{-15} to 10^{-7} g/ml in artificial urine (AU). The inset shows the kinetics of the reflectivity signal on the injection of AU as measured at a light incident angle of 70°.

might be ascribed to a small swelling of the MIF in AU. Accordingly, the affinity binding of testosterone on the macroporous MIF was carried out in AU, as indicated in the time-dependent reflectivity changes (Fig. 5B). The reflectivity increases up to $\Delta R = 2.5\%$ on the incubation of testosterone at concentrations up to 10^{-7} g/ml, which is lower than $\Delta R = 2.9\%$ as performed in PBS (Fig. 4A). The lower sensor response in AU than in PBS might be ascribed to the higher ionic strength and lower pH value of AU that weaken the affinity binding between the testosterone and the polymer matrix.

In addition, considering the presence of testosterone in human urine samples, we investigated the unspecific adsorption of human urine on the macroporous NIF sensor chips. The SPR reflectivity increased by up to 0.5% after the injection of the male and female urine and decreased back to the original level after rinsing with PBS buffer (see Fig. S4 in supplementary material). The increase of the reflectivity might be ascribed to the nonspecific adsorption of the small amount of proteins in the human urine; however, it can be removed through rinsing with PBS buffer. It indicated the feasibility for the detection of testosterone in human urine with the macroporous MIF sensor chip.

LOD for detection of testosterone

The calibration curve for the detection of testosterone in PBS and AU shows the SPR reflectivity changes as a function of the testosterone concentrations from 10^{-15} to 10^{-7} g/ml in Fig. 6. The reflectivity changes show good linearity versus logarithmic concentrations of the testosterone with the slopes around $S = 0.3\%$ ($\Delta R = 4.795 + 0.298\lg C$, $R^2 = 0.983$ and $\Delta R = 4.559 + 0.292\lg C$, $R^2 = 0.990$ for PBS and AU, respectively). The error bars obtained from three different chips in the calibration curve indicated good reproducibility of the macroporous MIF for the sensing of testosterone in PBS buffer and AU. The LOD for the detection of testosterone was estimated to be 10^{-15} g/ml (i.e., 3.5 fM) in PBS and AU. The LOD was determined as the concentration of testosterone at which the response is 3 times the standard deviation of the reflectivity baseline while taking the error bars into account (Fig. 6). As compared with the other molecular imprinting methods in doping analysis, liquid chromatographic and competitive immunoassay for the detection of testosterone with LODs of 0.3 ng/ml [45], 2 ng/ml [46], and 12 pg/ml [47], the SPR sensor based on this macroporous MIF provides more than four orders of magnitude lower detection limit. Furthermore, in comparison with other technologies such as conventional enzyme-linked immunosorbent assay (ELISA) and competitive immunoassays, this method provides direct detection of small molecules without using antibodies within short assay time (30 min). However, it also has limitations on the detection of various samples with high throughput as compared with other technologies such as ELISA. In addition, the cross-reactivity of the sensor chip to estradiol in this method is rather high, and this needs to be improved in future work.

Sensor performance in human urine

The MIF sensor performance in human urine was investigated in female and male urine samples. As shown in Fig. 7, the reflectivity increased after injection of the human urine, indicating the presence of testosterone. Comparing the response and the initial slope of the binding curve with the kinetic curve in Fig. 5, we can estimate that the amount of testosterone in the female and male urine is in a range from 1 to 100 ng/ml, which is comparable to the reported testosterone level in human urine [48]. The higher response $\Delta R = 0.7\%$ for male urine indicated the higher amount of testosterone than the female urine. Interestingly, the female urine does not show significant difference of the refractive index with respect to the PBS buffer, whereas the male urine results in an abrupt increase in reflectivity, indicating a high concentration of ions and/or proteins. Note that urine samples vary from person to person and also relates to people's diets. The sensor response ΔR increased up to 0.9% after the urine samples were spiked with 10^{-7} g/ml testosterone. The response is comparable to the one shown in Fig. 5B. However, because of the high concentration of testosterone in urine and the high variations of the sensor response, it has limited sensitivity to detect concentration variations lower than 1 ng/ml in human urine. We expect that further optimization of the MIFs can be carried out to reduce the sensor variations and improve the sensitivity on the detection of testosterone in human urine.

Stability and reproducibility of MIF-based SPR sensor

To evaluate the stability and reproducibility of the macroporous MIF, the sensor chips were stored in an unsealed bottle at room temperature when they were not in use. It retained the same

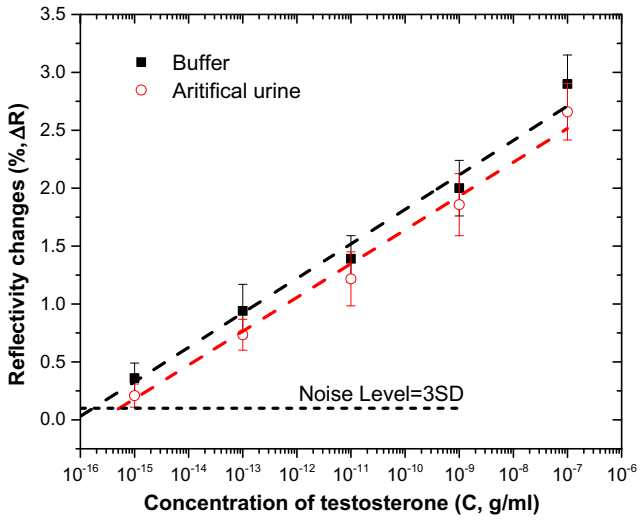

Fig.6. Calibration curves for the detection of testosterone in PBS buffer and artificial urine, as fitted with the linear function. The error bars were obtained from three different chips. 3SD, 3 standard deviations.

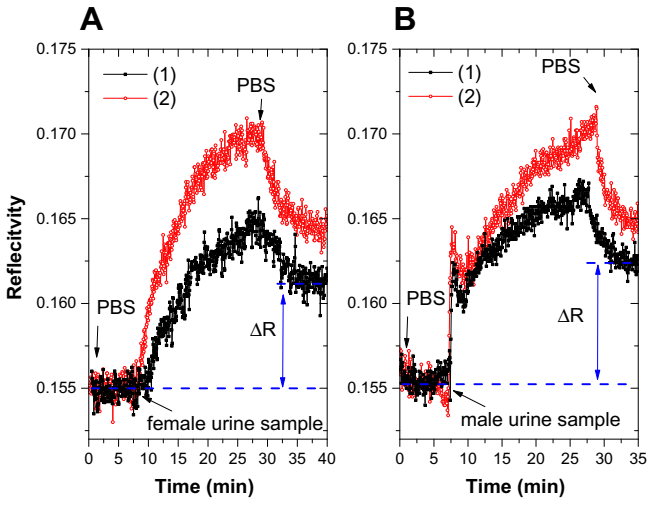

Fig.7. Time-dependent SPR reflectivity changes measured on the macroporous MIF on the incubation of female (left) and male (right) urine before (1) and after (2) being spiked with 10^{-7} g/ml testosterone.

angular reflectivity spectra and approximately 84% of its affinity to 10^{-15} g/ml testosterone in PBS after 8 months of storage (see Fig. S5 in supplementary material). These MIF-based sensors provided much better stability than typical antibody-based biosensors that survive only for days at room temperature. The fabrication of five sensor chips, made independently with different batches of bare gold chips, showed acceptable reproducibility with a relative standard deviation value of 27% for the affinity binding of testosterone at a concentration of 10^{-15} g/ml in PBS (Fig. S6).

Conclusions

A water-compatible macroporous MIF has been developed for SPR sensor on the sensitive detection of testosterone at a concentration as low as 10^{-15} g/ml in PBS and AU. The macroporous MIF achieved through the removal of PS NPs from the polymer matrix shows high sensitivity and accessibility for the binding of testosterone as compared with conventional MIF. Furthermore, this macroporous MIF demonstrated good selectivity for the binding of testosterone with respect to analogues such as progesterone and estradiol. Incubation of AU and human urine on the polymer films showed undetectable nonspecific adsorption. The sensor performance in female and male human urine indicated the feasibility for the detection of testosterone in human urine. In addition, this SPR sensor reveals high stability and reproducibility over 8 months of storage at room temperature without any specific protection. This method is a great candidate for rapid, simple, and label-free detection of molecules in aqueous solution such as hormones, stimulants, and other small molecules.

Acknowledgments

This research was supported by the National Natural Science Foundation of China (20771015) and the National "111" Project of China's Higher Education (B07012).

Appendix A. Supplementary data

Supplementary data associated with this article can be found, in the online version, at http://dx.doi.org/10.1016/j.ab.2014.06.014.

References

[1] M.J. Whitcombe, I. Chianella, L. Larcombe, S.A. Piletsky, J. Noble, R. Porter, A. Horgan, The rational development of molecularly imprinted polymer-based sensors for protein detection, Chem. Soc. Rev. 40 (2011) 1547–1571.
[2] B. Tse Sum Bui, K. Haupt, Molecularly imprinted polymers: synthetic receptors in bioanalysis, Anal. Bioanal. Chem. 398 (2010) 2481–2492.
[3] A. Lim, L. Trautmann, M.A. Peyrat, C. Couedel, F. Davodeau, F. Romagne, P. Kourilsky, M. Bonneville, Frequent contribution of T cell clonotypes with public TCR features to the chronic response against a dominant EBV-derived epitope: application to direct detection of their molecular imprint on the human peripheral T cell repertoire, J. Immunol. 165 (2000) 2001–2011.
[4] A. Katz, M.E. Davis, Molecular imprinting of bulk, microporous silica, Nature 403 (2000) 286–289.
[5] L. Chen, S. Xu, J. Li, Recent advances in molecular imprinting technology: current status, challenges, and highlighted applications, Chem. Soc. Rev. 40 (2011) 2922–2942.
[6] G. Vlatakis, L.I. Andersson, R. Muller, K. Mosbach, Drug assay using antibody mimics made by molecular imprinting, Nature 361 (1993) 645–647.
[7] T. Kitade, K. Kitamura, T. Konishi, S. Takegami, T. Okuno, M. Ishikawa, M. Wakabayashi, K. Nishikawa, Y. Muramatsu, Potentiometric immunosensor using artificial antibody based on molecularly imprinted polymers, Anal. Chem. 76 (2004) 6802–6807.
[8] J. Matsui, S. Goji, T. Murashima, D. Miyoshi, S. Komai, A. Shigeyasu, T. Kushida, T. Miyazawa, T. Yamada, K. Tamaki, N. Sugimoto, Molecular imprinting under molecular crowding conditions: an aid to the synthesis of a high-capacity polymeric sorbent for triazine herbicides, Anal. Chem. 79 (2007) 1749–1757.
[9] J. Matsui, K. Akamatsu, S. Nishiguchi, D. Miyoshi, H. Nawafune, K. Tamaki, N. Sugimoto, Composite of Au nanoparticles and molecularly imprinted polymer as a sensing material, Anal. Chem. 76 (2004) 1310–1315.
[10] J. Matsui, K. Akamatsu, N. Hara, D. Miyoshi, H. Nawafune, K. Tamaki, N. Sugimoto, SPR sensor chip for detection of small molecules using molecularly imprinted polymer with embedded gold nanoparticles, Anal. Chem. 77 (2005) 4282–4285.
[11] G. Wulff, Enzyme-like catalysis by molecularly imprinted polymers, Chem. Rev. 102 (2002) 1–27.
[12] J.O. Rich, V.V. Mozhaev, J.S. Dordick, D.S. Clark, Y.L. Khmelnitsky, Molecular imprinting of enzymes with water-insoluble ligands for nonaqueous biocatalysis, J. Am. Chem. Soc. 124 (2002) 5254–5255.
[13] A. Afkhami, H. Ghaedi, T. Madrakian, M. Ahmadi, H. Mahmood-Kashani, Fabrication of a new electrochemical sensor based on a new nano-molecularly imprinted polymer for highly selective and sensitive determination of tramadol in human urine samples, Biosens. Bioelectron. 44 (2013) 34–40.
[14] P. Cakir, A. Cutivet, M. Resmini, B.T. Bui, K. Haupt, Protein-size molecularly imprinted polymer nanogels as synthetic antibodies, by localized polymerization with multi-initiators, Adv. Mater. 25 (2013) 1048–1051.
[15] H. Bao, T.X. Wei, X.L. Li, Z. Zhao, H. Cui, P. Zhang, Detection of TNT by a molecularly imprinted polymer film-based surface plasmon resonance sensor, Chin. Sci. Bull. 57 (2012) 2102–2105.
[16] L. Fang, S. Chen, X. Guo, Y. Zhang, H. Zhang, Azobenzene-containing molecularly imprinted polymer microspheres with photo- and thermoresponsive template binding properties in pure aqueous media by atom transfer radical polymerization, Langmuir 28 (2012) 9767–9777.
[17] F. Horemans, J. Alenus, E. Bongaers, A. Weustenraed, R. Thoelen, J. Duchateau, L. Lutsen, D. Vanderzande, P. Wagner, T.J. Cleij, MIP-based sensor platforms for the detection of histamine in the nano- and micromolar range in aqueous media, Sens. Actuat. B 148 (2010) 392–398.
[18] G.Q. Pan, Y. Zhang, X.Z. Guo, C.X. Li, H.Q. Zhang, An efficient approach to obtaining water-compatible and stimuli-responsive molecularly imprinted polymers by the facile surface-grafting of functional polymer brushes via RAFT polymerization, Biosens. Bioelectron. 26 (2010) 976–982.
[19] B. Dirion, Z. Cobb, E. Schillinger, L.I. Andersson, B. Sellergren, Water-compatible molecularly imprinted polymers obtained via high-throughput synthesis and experimental design, J. Am. Chem. Soc. 125 (2003) 15101–15109.
[20] F. Horemans, A. Weustenraed, D. Spivak, T.J. Cleij, Towards water compatible MIPs for sensing in aqueous media, J. Mol. Recognit. 25 (2012) 344–351.
[21] X.B. Hu, Q. An, G.T. Li, S.Y. Tao, B. Liu, Imprinted photonic polymers for chiral recognition, Angew. Chem. Int. Ed. 45 (2006) 8145–8148.
[22] Y.X. Zhang, P.Y. Zhao, L.P. Yu, Highly-sensitive and selective colorimetric sensor for amino acids chiral recognition based on molecularly imprinted photonic polymers, Sens. Actuat. B 181 (2013) 850–857.
[23] J. Homola, Surface plasmon resonance sensors for detection of chemical and biological species, Chem. Rev. 108 (2008) 462–493.
[24] G. Gupta, P.K. Sharma, B. Sikarwar, S. Merwyn, S. Kaushik, M. Boopathi, G.S. Agarwal, B. Singh, Surface plasmon resonance immunosensor for the detection of *Salmonella typhi* antibodies in buffer and patient serum, Biosens. Bioelectron. 36 (2012) 95–102.
[25] Y. Wang, J. Dostalek, W. Knoll, Magnetic nanoparticle-enhanced biosensor based on grating-coupled surface plasmon resonance, Anal. Chem. 83 (2011) 6202–6207.
[26] V.M. Gaspar, C. Cruz, J.A. Queiroz, C. Pichon, I.J. Correia, F. Sousa, Sensitive detection of peptide–minicircle DNA interactions by surface plasmon resonance, Anal. Chem. 85 (2013) 2304–2311.
[27] Y. Wang, W. Knoll, J. Dostalek, Bacterial pathogen surface plasmon resonance biosensor advanced by long range surface plasmons and magnetic nanoparticle assays, Anal. Chem. 84 (2012) 8345–8350.
[28] R. D'Agata, G. Spoto, Surface plasmon resonance imaging for nucleic acid detection, Anal. Bioanal. Chem. 405 (2013) 573–584.
[29] J.S. Mitchell, T.E. Lowe, Ultrasensitive detection of testosterone using conjugate linker technology in a nanoparticle-enhanced surface plasmon resonance biosensor, Biosens. Bioelectron. 24 (2009) 2177–2183.
[30] M. Riskin, R. Tel-Vered, O. Lioubashevski, I. Willner, Ultrasensitive surface plasmon resonance detection of trinitrotoluene by a bis-aniline-cross-linked Au nanoparticles composite, J. Am. Chem. Soc. 131 (2009) 7368–7378.
[31] J. Ricanyova, R. Gadzala-Kopciuch, K. Reiffova, Y. Bazel, B. Buszewski, Molecularly imprinted adsorbents for preconcentration and isolation of progesterone and testosterone by solid phase extraction combined with HPLC, Adsorption 16 (2010) 473–483.
[32] H.N. Bui, P.M. Sluss, S. Blincko, D.L. Knol, M.A. Blankenstein, A.C. Heijboer, Dynamics of serum testosterone during the menstrual cycle evaluated by daily measurements with an ID–LC–MS/MS method and a 2nd generation automated immunoassay, Steroids 78 (2013) 96–101.
[33] G. Brandhorst, F. Streit, J. Kratzsch, J. Schiettecatte, H.J. Roth, P.B. Luppa, A. Korner, W. Kiess, L. Binder, M. Oellerich, N. von Ahsen, Multicenter evaluation of a new automated electrochemiluminescence immunoassay for the quantification of testosterone compared to liquid chromatography tandem mass spectrometry, Clin. Biochem. 44 (2011) 264–267.
[34] H. Kataoka, K. Ehara, R. Yasuhara, K. Saito, Simultaneous determination of testosterone, cortisol, and dehydroepiandrosterone in saliva by stable isotope dilution on-line in-tube solid-phase microextraction coupled with liquid chromatography–tandem mass spectrometry, Anal. Bioanal. Chem. 405 (2013) 331–340.
[35] X. de la Torre, C. Colamonici, D. Curcio, F. Molaioni, F. Botre, A comprehensive procedure based on gas chromatography–isotope ratio mass spectrometry following high performance liquid chromatography purification for the

analysis of underivatized testosterone and its analogues in human urine, Anal. Chim. Acta 756 (2012) 23–29.
[36] R.B. Pernites, R.R. Ponnapati, R.C. Advincula, Surface plasmon resonance (SPR) detection of theophylline via electropolymerized molecularly imprinted polythiophenes, Macromolecules 43 (2010) 9724–9735.
[37] M. Riskin, Y. Ben-Amram, R. Tel-Vered, V. Chegel, J. Almog, I. Willner, Molecularly imprinted Au nanoparticles composites on Au surfaces for the surface plasmon resonance detection of pentaerythritol tetranitrate, nitroglycerin, and ethylene glycol dinitrate, Anal. Chem. 83 (2011) 3082–3088.
[38] Y. Wang, C.J. Huang, U. Jonas, T.X. Wei, J. Dostalek, W. Knoll, Biosensor based on hydrogel optical waveguide spectroscopy, Biosens. Bioelectron. 25 (2010) 1663–1668.
[39] A.W. Martinez, S.T. Phillips, E. Carrilho, S.W. Thomas, H. Sindi, G.M. Whitesides, Simple telemedicine for developing regions: camera phones and paper-based microfluidic devices for real-time, off-site diagnosis, Anal. Chem. 80 (2008) 3699–3707.
[40] Q.W. Zhang, Y. Wang, A. Mateescu, K. Sergelen, A. Kibrom, U. Jonas, T.X. Wei, J. Dostalek, Biosensor based on hydrogel optical waveguide spectroscopy for the detection of 17-estradiol, Talanta 104 (2013) 149–154.
[41] Y. Wang, A. Brunsen, U. Jonas, J. Dostalek, W. Knoll, Prostate specific antigen biosensor based on long range surface plasmon-enhanced fluorescence spectroscopy and dextran hydrogel binding matrix, Anal. Chem. 81 (2009) 9625–9632.
[42] G.E. Perlmann, L.G. Longsworth, The specific refractive increment of some purified proteins, J. Am. Chem. Soc. 70 (1948) 2719–2724.
[43] T. Tumolo, L. Angnes, M.S. Baptista, Determination of the refractive index increment (dn/dc) of molecule and macromolecule solutions by surface plasmon resonance, Anal. Biochem. 333 (2004) 273–279.
[44] N. Gao, J. Dong, M. Liu, B. Ning, C. Cheng, C. Guo, C. Zhou, Y. Peng, J. Bai, Z. Gao, Development of molecularly imprinted polymer films used for detection of profenofos based on a quartz crystal microbalance sensor, Analyst 137 (2012) 1252–1258.
[45] B. Tse Sum Bui, F. Merlier, K. Haupt, Toward the use of a molecularly imprinted polymer in doping analysis: selective preconcentration and analysis of testosterone and epitestosterone in human urine, Anal. Chem. 82 (2010) 4420–4427.
[46] L. Konieczna, A. Plenis, I. Oledzka, P. Kowalski, T. Baczek, Optimization of LC method for the determination of testosterone and epitestosterone in urine samples in view of biomedical studies and anti-doping research studies, Talanta 83 (2011) 804–814.
[47] M. Sun, J. Manolopoulou, A. Spyroglou, F. Beuschlein, C. Hantel, Z. Wu, M. Bielohuby, A. Hoeflich, C. Liu, M. Bidlingmaier, A microsphere-based duplex competitive immunoassay for the simultaneous measurements of aldosterone and testosterone in small sample volumes: validation in human and mouse plasma, Steroids 75 (2010) 1089–1096.
[48] D.J. Borts, L.D. Bowers, Direct measurement of urinary testosterone and epitestosterone conjugates using high-performance liquid chromatography/tandem mass spectrometry, J. Mass Spectrom. 35 (2000) 50–61.